# RENORMALIZATION AND UNIVERSALITY IN DYNAMICS

RYAN O'FARRELL

Abstract. This paper will build up the theory of renormalization in dynamical systems of real and complex functions. Two main results are showcased: first, a proof of the Feigenbaum universality, and second, the presence of mini-Mandelbrots in the Mandelbrot set. We conclude with an exposition of the MLC conjecture.

## Contents



## 1. Introduction: A Fibonacci Mystery

Let's make a sequence. Start with any two numbers $a_1$ and $a_2$, and for all other terms let $a_n = a_{n-1} + a_{n-2}$. For example, if $a_1 = a_2 = 1$, the sequence would look like

$$1, 1, 2, 3, 5, 8, 13 \dots$$

This is the *Fibonacci sequence*. But the sequence could have also looked like

$$17, 29, 46, 75, 121, 196, 317 \dots$$

or

$$1, 1000, 1001, 2001, 3002, 5003, 8005 \dots$$

or any other sequence that follows the rule. If we take the ratio of successive terms in each sequence,

$$\frac{13}{8} = 1.625,\ \frac{317}{196} \approx 1.617,\ \frac{8005}{5003} \approx 1.600$$

they all seem to hover around 1.6. In fact, if we compute $a_{21}/a_{20}$,

$$\frac{10946}{6765} \approx 1.618034,\ \frac{267262}{165177} \approx 1.618034,\ \frac{6769181}{4183584} \approx 1.618034,$$

the ratio of successive terms seems to converge to a number that looks suspiciously like the *golden ratio* $\varphi = \frac{1+\sqrt{5}}{2}$. This phenomenon is an example of a *universality* result, where a large portion of the state space ends up tending towards the same limiting behavior. Why does this happen?

The answer has to do with *renormalization*, a technique originally from statistical physics that models how matter changes at different "scales". Let's say you want to model a material made of atoms.

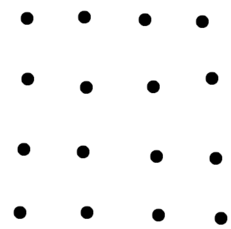

FIGURE 1. Any material, if you zoom in far enough.

Renormalization allows you to *coarse-grain*, or "block" groups of atoms together and treat them like single atoms. Effectively, we can "zoom out".

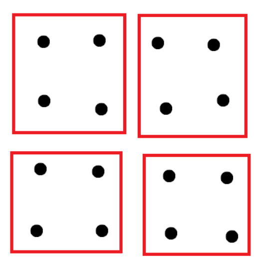

FIGURE 2. The coarse-graining procedure.

When you apply this procedure, your new "atoms" are going to behave differently from the old ones. Anything that looks like "noise" (like the microscopic "jiggling" of atoms above absolute zero) will become less and less noticeable as the blocks get bigger. Therefore, as we repeat this coarse-graining procedure, these effects will go to 0 in the macroscopic limit, so they are called *irrelevant observables*. However, *relevant observables* (most notably mass and volume, but also properties like magnetic field strength in magnetic materials) become larger and larger, so they stay relevant in the macroscopic limit. Renormalization lets us simplify problems by only considering these relevant parameters.

We can apply this idea to our problem by first encoding any of our sequences as a vector $\begin{bmatrix} a_2 \\ a_1 \end{bmatrix}$ consisting of our first two hand-picked entries. One way we might "zoom out" of our sequence is by starting it at the second term instead of the first. This will generate a new sequence that has the same end behavior as the first. We can define our *renormalization operator* $\mathcal{R}$ as the mapping

$$\begin{bmatrix} a_2 \\ a_1 \end{bmatrix} \mapsto \begin{bmatrix} a_3 \\ a_2 \end{bmatrix}.$$

By the nature of our sequence, we can actually write $\mathcal{R}$ as a matrix.

$$\mathcal{R} = \begin{bmatrix} 1 & 1 \\ 1 & 0 \end{bmatrix}$$

$$\mathcal{R} \begin{bmatrix} a_2 \\ a_1 \end{bmatrix} = \begin{bmatrix} 1 & 1 \\ 1 & 0 \end{bmatrix} \begin{bmatrix} a_2 \\ a_1 \end{bmatrix} = \begin{bmatrix} a_1 + a_2 \\ a_2 \end{bmatrix} = \begin{bmatrix} a_3 \\ a_2 \end{bmatrix}$$

What we mean by "the ratio of consecutive terms tends to $\varphi$" is that points under iteration tend towards the span of $\begin{bmatrix} \varphi \\ 1 \end{bmatrix}$. We call this line the *unstable manifold* of the system.

Wait, what? Why are points tending towards the *un*stable manifold? Isn't that backwards? It all has to do with the fixed point at the origin.

**Notation 1.1.** The notation $f^n$ refers to the $n$th *iteration* of $f$ and not function multiplication. The notation $f^{-n}(x)$ refers to the $n$th successive preimage of $x$ under $f$ (the set of all $y$ such that $f^n(y) = x$) and not $\frac{1}{f^n(x)}$.

**Definition 1.2.** The *unstable manifold*[1] of a fixed point $p$ of a function $f$ on a topological space $X$ is the set of all $q$ in $X$ such that $f^{-n}(q) \to p$ as $n \to \infty$.

**Definition 1.3.** The *stable manifold* of a fixed point $p$ of a function $f$ on a topological space $X$ is the set of all $q$ in $X$ such that $f^n(q) \to p$ as $n \to \infty$.

Points in the stable manifold have *future* iterations in a neighborhood of the fixed point, while points in the unstable manifold have *past* iterations in a neighborhood of the fixed point and future iterations away from it (hence, they are unstable). We can clarify the words "past" and "future" with the following definition.

**Definition 1.4.** The *forward orbit* of a point $x$ is the set $\bigcup_{n=0}^{\infty}\{f^n(x)\}$. The *backward orbit* of a point $x$ is the set $\bigcup_{n=0}^{\infty}\{f^{-n}(x)\}$. The *(complete) orbit* of $x$ is the union of the forward and backward orbits of $x$.

A good idea is to look at the *eigenvectors* of our linear map, since they have their past and future iterations on the same span as themselves. We find two.

$$\vec{v}_1 = \begin{bmatrix} \varphi \\ 1 \end{bmatrix} \text{ with } \lambda_1 = \varphi.$$

$$\vec{v}_2 = \begin{bmatrix} -1 \\ \varphi \end{bmatrix} \text{ with } \lambda_2 = 1 - \varphi.$$

Note that the iterations of $\mathcal{R}$ push $\vec{v}_1$ away from the fixed point and $\vec{v}_2$ towards the fixed point. This means that $\vec{v}_1$ is on the unstable manifold and $\vec{v}_2$ is on the stable manifold.

These observations hint at a much more general fact about stable and unstable manifolds which will be important in section 3. Most renormalization operators are not linear and so do not have eigenvectors. However, any differentiable function $f$ can be approximated by a linear operator in the neighborhood of a fixed point by the derivative. We therefore have

[1]There are some technical restrictions on our function and our space to ensure that these are manifolds. In this case, they're lines, and there's nothing more "manifoldy" than that.

**Key Idea 1.5.** The dimensionality and direction of the stable and unstable manifolds around a fixed point of $f$ are determined by the eigenvectors of the derivative $Df$. Each eigenvector with $\lambda > 1$ corresponds to a dimension of the unstable manifold, and each eigenvector with $\lambda < 1$ corresponds to a dimension of the stable manifold.

We can visualize our stable and unstable manifolds with the *renormalization group flow*,[2] which shows how different points behave under iteration.

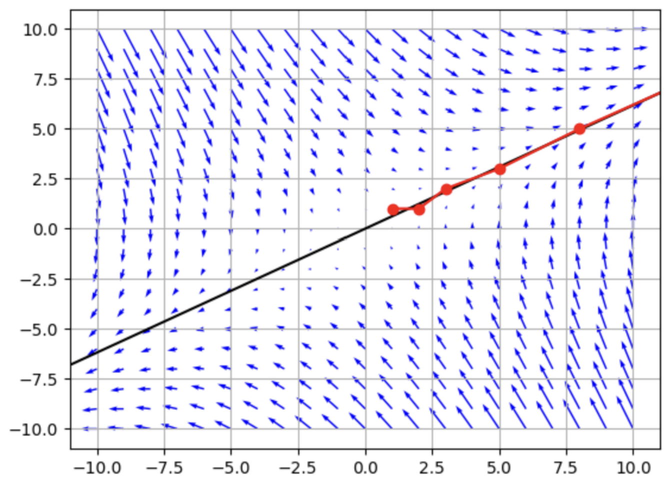


FIGURE 3. Renormalization group flow visualized, plotted with $\operatorname{Span}\left(\begin{bmatrix}\varphi\\1\end{bmatrix}\right)$ (black) and the forward orbit of $\begin{bmatrix}1\\1\end{bmatrix}$ (red)

It really does appear that points tend towards the unstable manifold under iteration. To prove this once and for all and finally solve our $\varphi$ mystery, we just need to write our sequences in terms of our eigenvalues. Since our eigenvectors form a basis, we can write any sequence vector $a$ as $c_1\vec{v}_1 + c_2\vec{v}_2$. If $c_1 \neq 0$,[3] then we have for sufficiently large $n$ that

$$\mathcal{R}^n a = c_1\varphi^n\vec{v}_1 + c_2(1-\varphi)^n\vec{v}_2 \approx c_1\varphi^n\vec{v}_1$$

which is in the span of $\vec{v}_1 = \begin{bmatrix}\varphi\\1\end{bmatrix}$. Thus, for almost every sequence, the ratio of consecutive terms tends to $\varphi$. This is again indicative of a general theme of renormalization.

**Key Idea 1.6.** Almost every point under iteration by $f$ tends toward the unstable manifold of $f$.

Since the dimensionality of the unstable manifold is often much less than the whole space, renormalization leads to *universality* results, from macroscopic objects not needing to be described by the motions of individual atoms to the *Feigenbaum universality*, which will be described in the next few sections.

---

[2]Nothing to do with group theory. Blame the physicists.

[3]If you happened to choose the sequence $(-\varphi, 1, \dots)$ at the beginning and were wondering why it converged to $-\varphi^{-1}$ instead, I'm sorry.

## 2. The Logistic Map

Consider the family of functions $f_r : [0,1] \to [0,1]$ with $r \in [0,4]$ defined by

$$f_r(x) = rx(1-x) \tag{2.1}$$

This map is called the *logistic map*, so named because it can be thought of as the discrete analog of the *logistic differential equation* $y' = ry(1-y)$. What happens when you iterate $f_r$? The answer ends up being very sensitive to your choice of $r$.

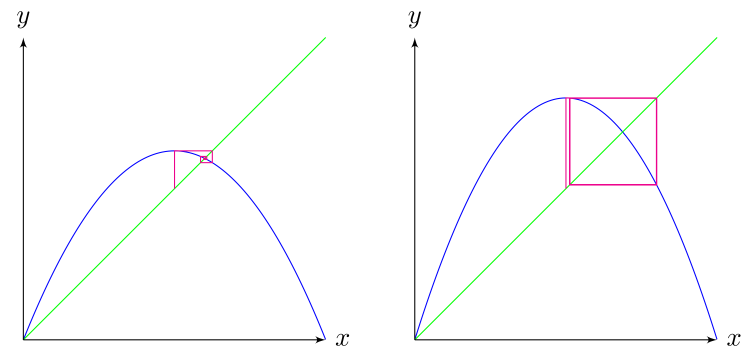


(A) $r = 2.5$. Attracting fixed point. (B) $r = 3.2$. Attracting 2-cycle.

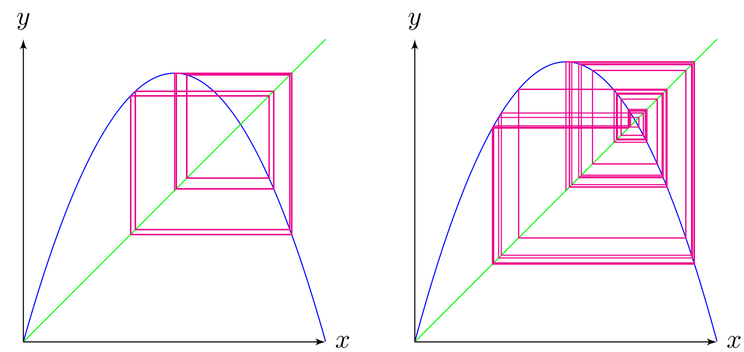


(C) $r = 3.55$. Attracting 8-cycle. (D) $r = 3.7$. Chaos.

Figure 4. Cobweb plots for different values of $r$, featuring $y = x$ (green), $y = f_r(x)$ (blue) and the forward orbit of $\frac{1}{2}$ (magenta).

**Definition 2.2.** A point $x$ is part of an *$n$-cycle* if $n$ is the smallest positive integer such that $f^n(x) = x$. We say the cycle has period $n$ and $x$ is $n$-periodic.

**Definition 2.3.** $x$ is a *fixed point* if it is 1-periodic.

**Definition 2.4.** An $n$-cycle is *attracting* if for any $x$ in the cycle $|(f^n)'(x)| < 1$, *repelling* if $|(f^n)'(x)| > 1$ and *indifferent* if $|(f^n)'(x)| = 1$.

**Remark 2.5.** Attracting cycles "pull" nearby points "in", while repelling cycles "push" nearby points "away". This is because if $x$ is $n$-periodic then for a sufficiently nearby point $y$

$$|f^n(y) - x| = |f^n(y) - f^n(x)| \approx |(f^n)'(x)||y - x|$$

so if the cycle is attracting $|f^n(y) - x| < |y - x|$ and if repelling $|f^n(y) - x| > |y - x|$.

**Theorem 2.6.** *For $r \in [0,1)$ , $f_r$ has an attracting fixed point at 0. Moreover, every point $x \in [0,1]$ tends toward 0 under iteration.*

*Proof.* Note that $f_r(0) = 0$ and $|f_r'(0)| = r < 1$. To finish off the proof, it suffices to see that $0 \leq f_r(x) \leq rx < x$, so $0 \leq f_r^n(x) \leq r^n x \to 0$, guaranteeing convergence. $\square$

This result also holds for $r = 1$, with the exception that 0 is an indifferent fixed point. However, we start to get different behavior when $r > 1$.

**Theorem 2.7.** *For $r \in (1,3)$ , $f_r$ has a repelling fixed point at 0 and an attracting fixed point at $\frac{r-1}{r}$.*

*Proof.* With the tools presented so far, this follows from straightforward computation. $\square$

When talking about limits under iteration, generally we care much more about attracting cycles compared to repelling ones. This is because, unlike attracting cycles, repelling cycles are highly sensitive to our initial conditions. Thus, although our function technically has two fixed points, the set which tends to 0 (which is just $\{0,1\}$) does not need to be considered.

Is it true, though, that every other point tends to $\frac{r-1}{r}$? How do we know there isn't an attracting cycle of any other period hiding somewhere? The easiest way to answer this question is to break out an incredibly powerful tool from complex dynamics.

**Definition 2.8.** A *critical point* of a differentiable function $f$ is a point $z$ where $f'(z) = 0$.

**Theorem 2.9.** *For every attracting cycle of a polynomial $f : \hat{\mathbb{C}} \to \hat{\mathbb{C}}$ with degree $\geq 2$ there exists a critical point that falls into it.*

Further discussion of complex dynamics (including a proof of Theorem 2.9) will be in section 4. Since our function is restricted to mapping $[0,1]$ into itself, and there is only one critical point of $f_r$ in $[0,1]$ (namely, $\frac{1}{2}$), we know there is only one attracting cycle, and it's the period 1 one we already found.

We can begin to plot the attracting behavior of $f_r$ for different values of $f$. For $r \in [0,1]$ we'll plot 0 and for $r \in (1,3]$ we'll plot $\frac{r-1}{r}$.

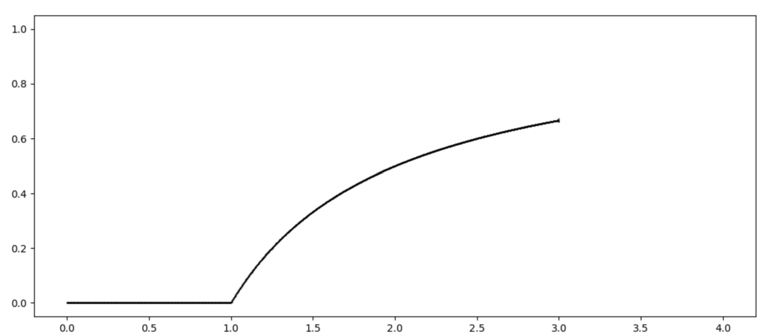


FIGURE 5. The first part of our plot, with $0 \leq r \leq 3$.
$r$ value ($x$-axis) plotted against attracting points ($y$-axis).

Let's keep going. Something interesting happens again for $r > 3$, since our fixed point at $\frac{r-1}{r}$ is no longer attracting. However, we start getting an attracting 2-cycle. If we look at $f_r^2(x)$, we find two additional attracting fixed points.

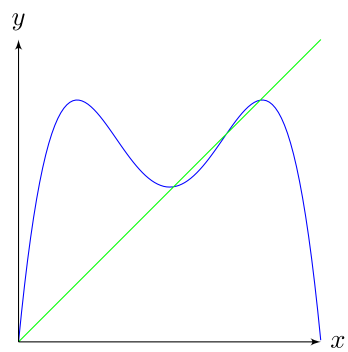


FIGURE 6. $y = f_{3.2}^2(x)$. Two attracting fixed points.

Since our critical point falls into this cycle, the 2-cycle is the only attracting end behavior. In fact, we can take a closer look at our critical point.

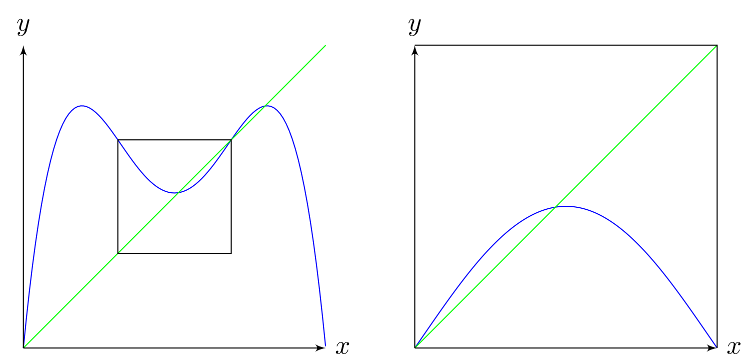


FIGURE 7. The right plot is a scaled and rotated version of the left plot $y = f_{3.2}^2(x)$.

The scaled and rotated plot looks kind of like $f_{r'}$ for a smaller value $r'$! There's a similarity between $f_r^2$ and a scaled version of a different $f_r$, which means we can try applying our coarse-graining procedure from Section 1. Instead of looking at one iteration at a time, we can look at iterations of $f_r^2$.

Let's formalize what it means for a map to be "like" another map.

**Definition 2.10.** A function $f$ is *conjugate* to another function $g$ if there exists a map $T$ of the form $z \mapsto \frac{az+b}{cz+d}$ with $ad - bc \neq 0$ such that $g = T \circ f \circ T^{-1}$.

Maps like $T$ are called *Möbius transformations* and they play a very important role in complex dynamics (Theorem 4.2). Of importance to us is that $T$ can be a linear (affine) function if $c = 0$.

**Theorem 2.11.** *If $f$ is conjugate to $g$ then $g$ is conjugate to $f$.*

**Remark 2.12.** Conjugate maps have "the same dynamics" in the sense that for all $n$, $g^n = T \circ f^n \circ T^{-1}$, so there is an easy map between the orbits of points under $f$ and under $g$.

We'll want to find a conjugacy map that sends the key features of $f_r^2$ to the key features of $f_{r'}$. Both $f_r^2$ and $f_{r'}$ have critical points at $\frac{1}{2}$, so that should be a fixed point of $T$. Then, note that $f_r^2$ has a repelling fixed point at $\frac{r-1}{r}$, so that should be mapped to the repelling fixed point at 0 of $f_{r'}$. In the end we can define our map as follows:

$$T : x \mapsto \frac{1}{2-r}(xr - r + 1), T^{-1} : x \mapsto \left(\frac{2}{r} - 1\right) x - \frac{1}{r} + 1, \tag{2.13}$$

$$(\mathcal{R} f_r^2)(x) = T(f_r^2(T^{-1}(x))).$$

This new function is called a *renormalization* of $f_r^2$. There's one small problem with our renormalization: it's not quadratic. That is, it's not actually equal to $f_{r'}$ for any $r'$. We can work around this, though.

**Definition 2.14.** A *quadratic-like map* is a differentiable map $f : U \to U'$ such that

- $U$ and $U'$ are open and connected and $U$ is compactly contained in $U'$ (there exists an compact set K such that $U \subset K \subset U'$).
- $f$ contains a single critical point, and for all other points $f$ is a 2-to-1 mapping.

**Definition 2.15.** A quadratic polynomial $f$ is *renormalizable* if for some $f^n$ where $n > 1$ there is a domain restriction such that $f^n$ is a quadratic-like map.

When this quadratic-like map has an attracting fixed point, then our $f_r$ has an attracting cycle of period 2, so we can add that to our plot.

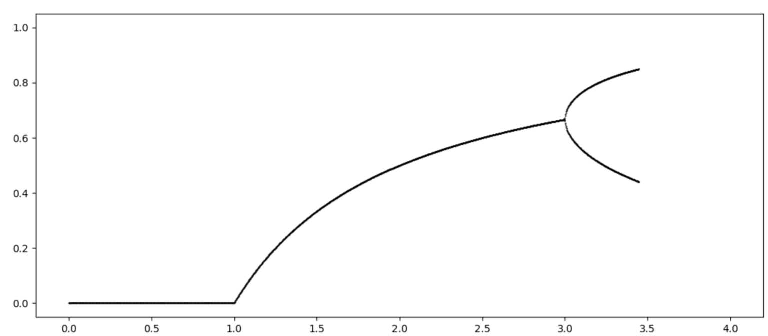


FIGURE 8. The 2-cycles.

For $r > 1 + \sqrt{6}$, the fixed point of the quadratic-like map becomes repelling. What happens next?

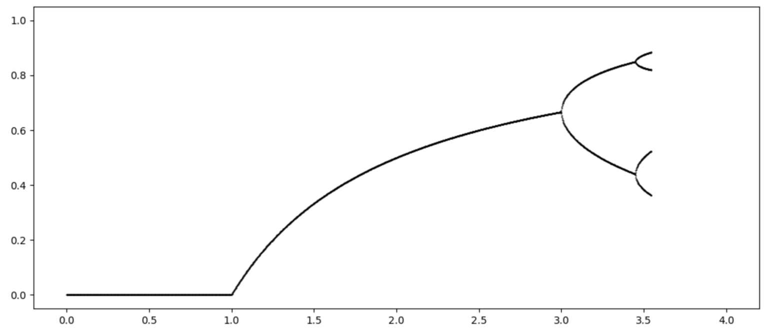


FIGURE 9. The 4-cycles.

Amazingly, just as our original fixed point of $f_r$ became a 2-cycle at $r = 3$, our fixed point of the renormalized quadratic-like map becomes a 2-cycle at $r = 1 + \sqrt{6}$, causing $f_r$ to have a 4-cycle. By coarse-graining in time, since our renormalized map is so close to the original map, the cycles just continue to double. Our 4-cycle becomes an 8-cycle, 16-cycle, and so on. This *period-doubling cascade* continues to infinity.

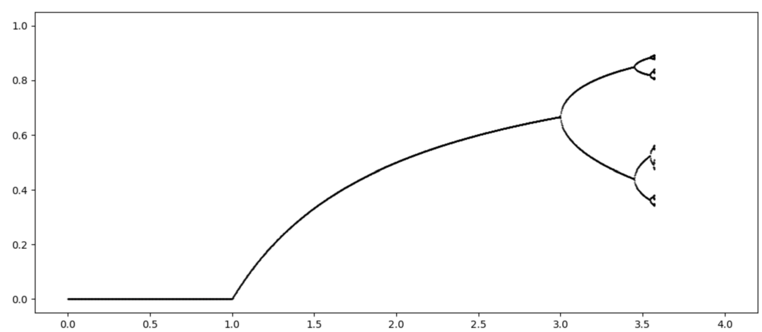


FIGURE 10. The period-doubling cascade.

"Infinity", as it turns out, occurs at $r \approx 3.56995$. After this point, chaos ensues.

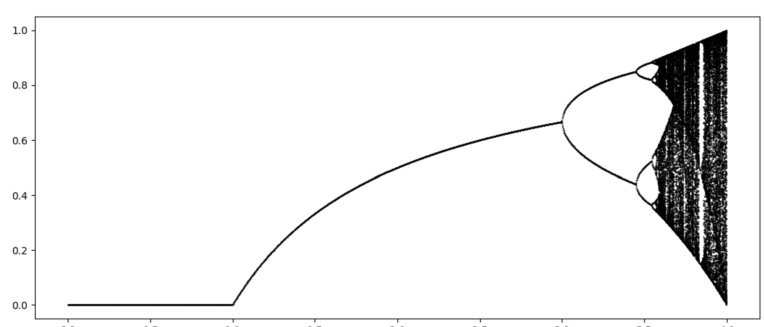


FIGURE 11. Our final plot.

There are points where there is a stable 3-cycle (visible in the plot), 5-cycle, or (as it turns out) $n$-cycle for any $n$, corresponding to points where $f_r^n$ is renormalizable. In fact, the set of parameters where there is a finite stable cycle is open and dense (Theorem 6.11). However, typically (measure-wise) there is no stable cycle at all, and this continues until $r = 4$, past which the interval $[0, 1]$ no longer maps into itself.

Let's take a closer look at that period-doubling cascade, though.

## 3. Feigenbaum Universality

In 1975, Mitchell Feigenbaum discovered something striking: if you measure the distance between two period doublings, the ratio of consecutive distances appeared to converge to a constant value $\delta = 4.669\ldots$

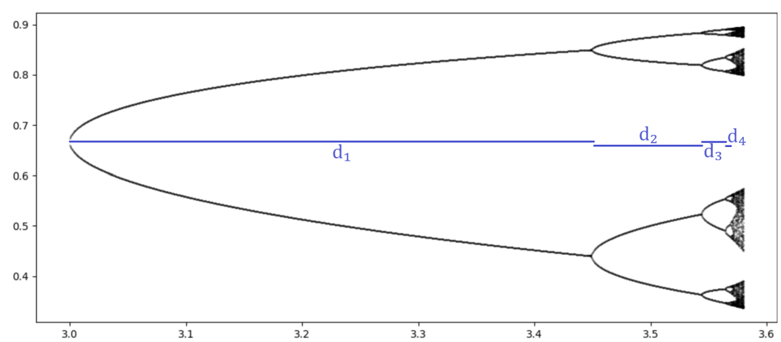


Figure 12. $\frac{d_n}{d_{n+1}} \to \delta \approx 4.669\ldots$

But wait, there's more! This same constant seemed to appear no matter which family of quadratic-like maps was considered.

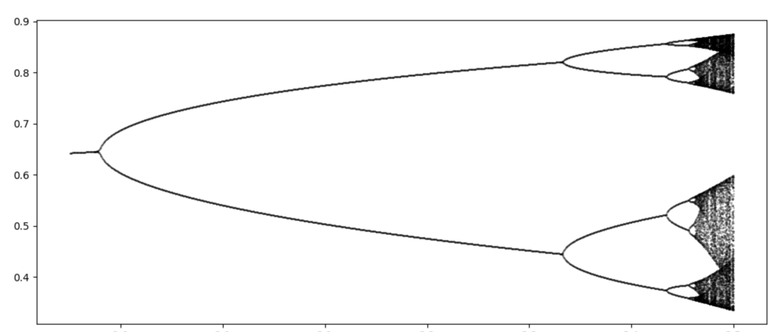


Figure 13. Bifurcation diagram for $g_r(x) = \frac{r}{4}\sin(\pi x)$. Notice the similarities.

Seeing this behavior, he proposed a set of conjectures that would explain it. To make sense of these conjectures, it would be a lot easier if our critical point was at 0. Fortunately,

**Theorem 3.1.** *A map of the form* $f_r(x) = rx(1-x)$ *with* $r > 2$ *is conjugate to exactly one map of the form* $g_\mu(x) = 1 - \mu x^2$ *with* $\mu = \frac{r^2}{4} - \frac{r}{2}$.

*Proof.* Verify that with

$$T(x) = \frac{2}{r-2}(2x-1)$$

we have that $g_\mu = T \circ f_r \circ T^{-1}$. □

We can then define a renormalization operator similar to (2.13) which acts on a very particular space.

**Notation 3.2.** Let $h$ be an analytic even map with $h(0) = 1$ and $xh'(x) < 0$. Denote by $\mathcal{B}$ the space of all such $h$.

Every $g_\mu$ is in $\mathcal{B}$, and in general elements of $\mathcal{B}$ are even and have a single "peak" at 0. If $h$ is renormalizable (in the sense of Definition 2.15) then we can define a renormalization operator $\mathcal{R}$ on $\mathcal{B}$ as follows:

$$(\mathcal{R}h)(x) = \frac{1}{h(1)}h^2(h(1)x)$$

Feigenbaum conjectured three things about $\mathcal{R}$, all of which were later proven.

**Theorem 3.3.** $\mathcal{R}$ *has an analytic fixed point* $\phi$.

**Theorem 3.4.** *The derivative of* $\mathcal{R}$ *at* $\phi$ *has one eigenvalue equal to* $\delta \approx 4.669 > 1$, *and all other eigenvalues lie in the open unit disk.*

Just as in Key Idea 1.5, this would imply that the unstable manifold $W_u$ is one-dimensional.

**Theorem 3.5.** *The unstable manifold intersects the space of functions* $h$ *such that* $h(1) = 0$ *transversally.*

Functions in this space are called *superstable*.

**Definition 3.6.** A quadratic-like map is called *superstable* if the critical point is part of an attracting cycle.

The proposed mechanism is follows. Theorem 3.3 guarantees that we have a fixed point $\psi$ of our renormalization operator in $\mathcal{B}$. By Theorem 3.4, we have a local unstable manifold of dimension 1 around our fixed point and a local stable manifold of codimension 1 (effectively the whole space minus one dimension). By Theorem 3.5 the unstable manifold extends to intersect the superstable manifold.

Now consider any family of functions that intersects both the stable and superstable manifold. The action of $\mathcal{R}$ on this family "drags" it closer to the unstable manifold. For any parameters sufficiently close to the fixed point along the unstable manifold, the action of $\mathcal{R}$ "stretches" it by a factor of $\delta$.

Consider the set of all parameters such that the function has an attracting $2^n$-cycle for $n \gg 1$. Sufficient iteration of $\mathcal{R}$ will map these parameters extremely close to the unstable manifold and to functions with $2^m$-cycles, with $1 \ll m < n$. Once sufficiently close to the unstable manifold, the action of $\mathcal{R}$ will both map these functions to functions with $2^{m-1}$-cycles and stretch them out by a factor of $\delta$. Therefore, no matter what the starting family is, the "width" of the parameters corresponding to $2^{m-1}$-cycles will always be $\delta = 4.669\ldots$ times greater than the "width" of the parameters corresponding to $2^m$-cycles.

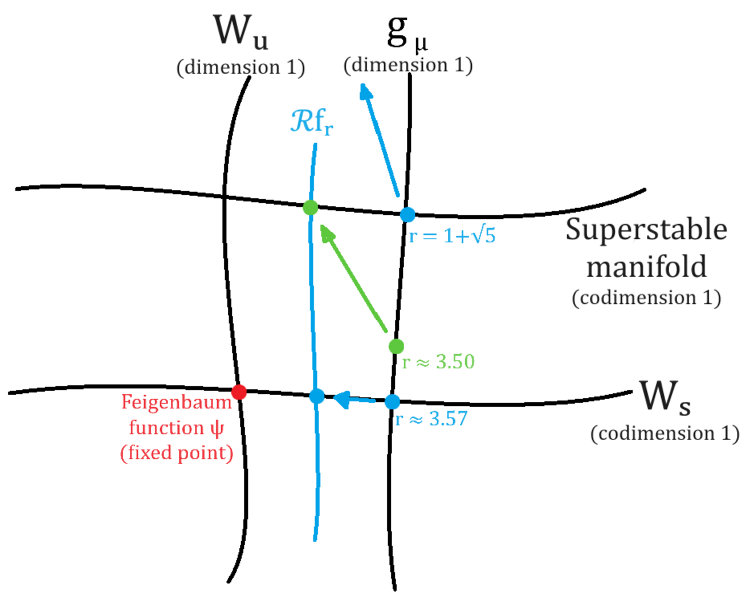


FIGURE 14. The action of $\mathcal{R}$ on our space.

The proofs presented here will mostly follow [2] with details filled in. The overall theme of these proofs is to first use a computer to approximate our desired property, and then use rigorous bounds and estimates to say "Well, it's got to be in there somewhere!"

*Proof of Theorem 3.3.* Our first step is to guess. We can use a computer to generate the polynomial

$$\psi_0(x) = 1 - (1.5276329970\ldots)x^2 + (0.1048151947\ldots)x^4 + \\ \cdots + (-2.7730511607\ldots \cdot 10^{-10})x^{20}$$

The full list of coefficients is [2].

This is pretty close to a fixed point. How close? Well, we first have to define a norm. We can associate any element $\psi$ of $\mathcal{B}$ to an element $(u, (v_n))$ of $(\mathbb{R} \times \ell^1)$ by the following:

$$\psi(x) = 1 - x^2 \left( \frac{u}{10} + \sum_{n=1}^{\infty} v_n \left( \frac{x^2 - 1}{2.5} \right)^n \right),$$

where we single out that first coefficient for convenience. We can then define the norm

$$|\psi| = |u| + \sum |v_n|$$

We need this weird norm because most norms aren't "strong enough" to give us the bounds we want. Specifically $\mathcal{B}$ is *complete* under this norm, which follows from the completeness of $\ell^1$. This fact will come in handy later.

Next, take the derivative of $\mathcal{R}$ at $\psi$.

Wait, what? Derivative of an operator? What does that mean? We can think of $\mathcal{R}$ as a function from $\mathbb{R} \times \ell^1$ to $\mathbb{R} \times \ell^1$. In this way, we can write $D\mathcal{R}$ as a (block) matrix

$$\begin{bmatrix} \alpha(\psi) & \beta(\psi) \\ \gamma(\psi) & \delta(\psi) \end{bmatrix}$$

where $\alpha$ is a real number, $\beta$ is a linear map $\ell^1 \to \mathbb{R}$, $\gamma$ is in $\ell^1$, and $\delta$ a linear map $\ell^1 \to \ell^1$.

To find a fixed point, we just need to solve $\mathcal{R}\psi - \psi = 0$. Inspired by Newton's method, we might take a look at the map

$$\tilde{\Phi}(\psi) = \psi - (D\mathcal{R} - \mathbb{1})^{-1}(\mathcal{R}\psi - \psi)$$

We can replace $D\mathcal{R}$ with the approximation

$$D\mathcal{R} \approx \begin{bmatrix} 4.669 & 0 \\ 0 & 0 \end{bmatrix} \implies (D\mathcal{R} - \mathbb{1})^{-1} \approx \begin{bmatrix} \frac{1}{3.669} & 0 \\ 0 & -\mathbb{1} \end{bmatrix} = J$$

and define

$$\Phi(\psi) = \psi - J(\mathcal{R}\psi - \psi).$$

Note that since $J$ is invertible, any fixed point of $\Phi$ must solve $\mathcal{R}\psi - \psi = 0$, so it must also be a fixed point of $\mathcal{R}$.

**Lemma 3.7.** *$\Phi$ is a contraction mapping on the ball $|\psi - \psi_0| \le 0.01$.*

*Proof.* Note that

$$D\Phi = \mathbb{1} - J(D\mathcal{R} - \mathbb{1}).$$

We're going to need to use two estimates that, while beyond the scope of this paper, can be obtained by very careful computing. The first one is

**Estimate 3.8.** *If $|\psi - \psi_0| < 0.01$ then $|\alpha - 4.669| < 0.148$, $|\beta| < 0.560$, $|\gamma| < .756$, and $|\delta| < .719$.*

Using careful calculation, we can find the *operator norm* of $D\Phi$.

**Definition 3.9.** The *operator norm* of $D\Phi$ is the maximum value of $\frac{|(D\Phi)(x)|}{|x|}$. In essence, it's the maximum "stretch" of the input values.

Writing $x = (u, v_n)$ we have that

$$\begin{aligned}
|(D\Phi)(x)| &= |(\mathbb{1} - J(D\mathcal{R} - \mathbb{1}))x)| \\
&= \left| \left( \mathbb{1} - \begin{bmatrix} \frac{1}{3.669} & 0 \\ 0 & -\mathbb{1} \end{bmatrix} \begin{bmatrix} \alpha - 1 & \beta \\ \gamma & \delta - \mathbb{1} \end{bmatrix} \right) \begin{bmatrix} u \\ v_n \end{bmatrix} \right| \\
&= \left| \left( \begin{bmatrix} 1 & 0 \\ 0 & \mathbb{1} \end{bmatrix} - \begin{bmatrix} \frac{\alpha-1}{3.669} & \frac{\beta}{3.669} \\ -\gamma & \mathbb{1} - \delta \end{bmatrix} \right) \begin{bmatrix} u \\ v_n \end{bmatrix} \right| \\
&= \left| \begin{bmatrix} \frac{4.669-\alpha}{3.669} & \frac{-\beta}{3.669} \\ \gamma & \delta \end{bmatrix} \begin{bmatrix} u \\ v_n \end{bmatrix} \right| \\
&= \left| \begin{bmatrix} \frac{4.669-\alpha}{3.669} u - \frac{\beta}{3.669} v_n \\ \gamma u + \delta v_n \end{bmatrix} \right| = \frac{1}{3.669} |(4.669 - \alpha)u - \beta v_n| + |\gamma u + \delta v_n| \\
&\le \frac{1}{3.669}(0.148|u| + 0.560|v_n|) + 0.756|u| + 0.719|v_n| \\
&< 0.9(|u| + |v_n|) = 0.9|x|.
\end{aligned}$$

so $|D\Phi| < 0.9$. Thus, $\Phi$ "squishes" the space by at least a factor of 0.9. To show that it is a contraction mapping, we just need to show that it maps the ball into itself, which can be shown by demonstrating that

$$\frac{|\Phi(\psi_0) - \psi_0|}{1 - 0.9} < 0.01$$

In fact, we have

**Estimate 3.10.** $|\Phi(\psi_0) - \psi_0| < 4 \cdot 10^{-6}$.

Since our guess $\psi_0$ is so close to a fixed point, $\Phi$ is indeed a contraction mapping, proving the lemma. $\square$

Since $\mathcal{B}$ is complete under this norm, by the Banach Fixed-Point Theorem and Lemma 3.7, we immediately know there is an analytic fixed point within the ball, proving Theorem 3.3. $\square$

*Proof of Theorem 3.4.* Seeing that $D\mathcal{R}$ has an expanding subspace is easy. Note that even with the worst-case estimate $|(D\mathcal{R})(1,0)| > |(1,0)|$. To see that this subspace is one-dimensional, consider the operator

$$\tilde{D} = \begin{bmatrix} \frac{1}{100} & 0 \\ 0 & \mathbb{1} \end{bmatrix} \begin{bmatrix} \alpha & \beta \\ \gamma & \delta \end{bmatrix} = \begin{bmatrix} \frac{\alpha}{100} & \frac{\beta}{100} \\ \gamma & \delta \end{bmatrix}.$$

In a similar way to the proof of Theorem 3.3 it can be seen that $\tilde{D}$ is a contraction mapping, so its spectrum is entirely contained in the unit disk. Since

$$\begin{bmatrix} 100 & 0 \\ 0 & \mathbb{1} \end{bmatrix}$$

only expands in one dimension, the operator

$$D\mathcal{R} = \begin{bmatrix} 100 & 0 \\ 0 & \mathbb{1} \end{bmatrix} \tilde{D}$$

can only expand in at most one dimension. $\square$

*Proof of Theorem 3.5.* In fact, it's possible to construct the unstable manifold explicitly. However, this relies on an entirely separate set of more complicated numerical estimates. Details are in [3]. With this last detail filled in, this completes the proof of the Feigenbaum conjectures. $\square$

## 4. Complex Dynamics

We're left with one dangling thread. What about the proof of Theorem 2.9? We're going to need to dive into the world of complex-valued functions.

The complex plane $\mathbb{C}$ is big. It would be nicer if there was a way to curl it up into something more manageable. Fortunately, we can use *stereographic projection*, which maps $\mathbb{C}$ to the unit sphere.

The idea is to place a unit sphere centered at 0 in the complex plane. To figure out where a point $Z$ on the plane maps to, draw a line from the north pole towards $Z$. This line intersects the sphere at exactly one place, which is the image under stereographic projection.

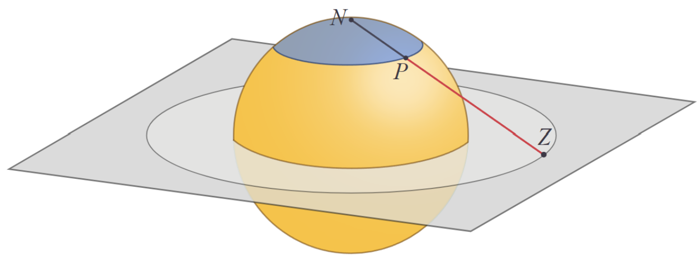


FIGURE 15. Stereographic projection maps $Z$ to $P$. [4]

If $Z = x + yi$, the image of $Z$ is given by

$$Z \mapsto \frac{1}{1+|Z|^2}(2x, 2y, |Z|^2 - 1) \in \mathbb{R}^3.$$

We don't get the *whole* sphere, though. We're missing the north pole, and something interesting happens when we fill it in. Any sequence that diverges (to infinity) in the complex plane *converges* on the sphere to the north pole. In a sense, the north pole acts like a "point at infinity".[4] What we've created is $\mathbb{C} \cup \{\infty\}$, called the *Riemann sphere* or $\hat{\mathbb{C}}$.

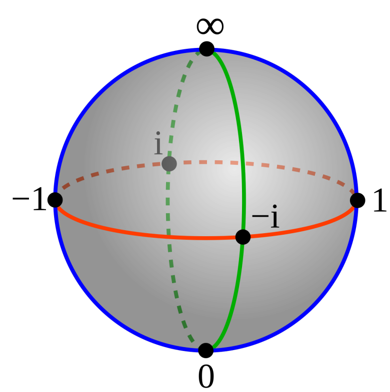


FIGURE 16. The Riemann sphere. [5]

What makes the stereographic projection nice is that it's *conformal*, which means it preserves angles and orientations. Conformal maps are very important in complex analysis for the following reason.

**Theorem 4.1.** *A map $f : U \subseteq \hat{\mathbb{C}} \to V \subseteq \hat{\mathbb{C}}$ is conformal at $z_0$ if it is holomorphic (complex differentiable, equivalently analytic) at $z_0$ and $f'(z_0) \neq 0$.*

*Proof.* What it means for a function to be holomorphic at $z_0$ is that in a neighborhood around $z_0$ it locally "looks like" multiplication by the complex number $f'(z_0)$,

---

[4] If you've been fed the lie that "infinity is not a number", I would recommend looking into *projective geometry*, a field which deals with $\infty$ just like any other number.

which when $f'(z_0) \neq 0$ "looks like" scaling and rotation, which are both conformal, which means that $f$ is locally a conformal map at $z_0$. $\square$

The Riemann sphere lets us see what's so special about Möbius transformations.

**Theorem 4.2.** *Möbius transformations are the only conformal homeomorphisms from $\hat{\mathbb{C}}$ to itself.*

*Proof.* We can see that they *are* conformal homeomorphisms by noting that if $f = \frac{az+b}{cz+d}$ with $ad - bc \neq 0$, then $f$ is bijective and differentiable with[5]

$$f^{-1}(z) = \frac{dz - b}{-cz + a}, f'(z) = \frac{ad - bc}{(cz + d)^2}.$$

Since $f'(z)$ exists and is nonzero everywhere (even at $\infty$), f is a conformal homeomorphism.

The proof that these are the *only* ones is trickier. The two key ingredients are

**Theorem 4.3.** *If $f : \hat{\mathbb{C}} \to \hat{\mathbb{C}}$ is a holomorphic map then $f$ is a rational function of the form $\frac{P(z)}{Q(z)}$, where $P$ and $Q$ are polynomials.*

**Definition 4.4.** The *degree* of a rational map is the maximum of the degrees of $P$ and $Q$

**Theorem 4.5.** *A rational map of degree $d$ has exactly $d$ preimages for every point up to multiplicity.*

These results will not be proven here, but together they rule out every other type of function from being a conformal homeomorphism. $\square$

Now that we have a sensible picture of "converging to infinity", we can take a look at what small neighborhoods look like under iteration. Some neighborhoods stay bounded while others don't.

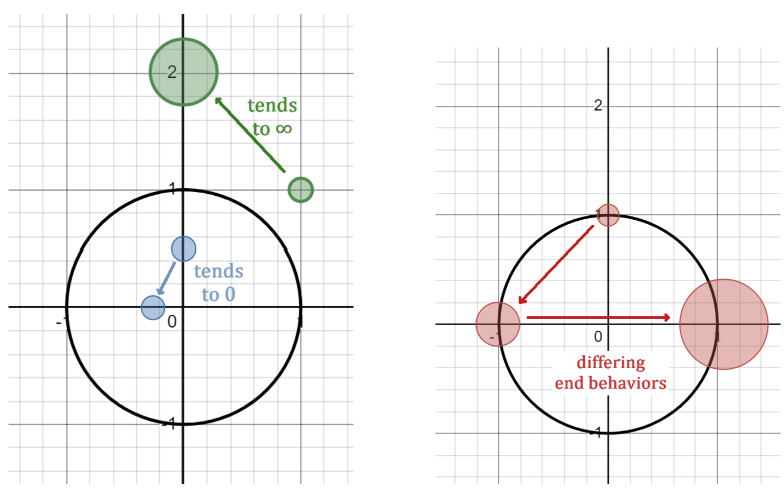


(A) Neighborhoods that stay bounded on the sphere.

(B) Neighborhoods that become unbounded.

FIGURE 17. Neighborhoods under iteration of $z \mapsto z^2$

[5]If these look "matrix-y" to you, you'd be right. The key word is PGL(2,$\mathbb{C}$).

We can formalize this with *equicontinuity*.

**Definition 4.6.** A family of functions $\{f_n\}$ is *equicontinuous* if for every $\epsilon > 0$, there exists one $\delta$ such that for *each* member of the family

$$d(x,y) < \delta \implies d(f_n(x), f_n(y)) < \epsilon.$$

The metric $d$ being used is the *chordal metric*, the straight-line distance through the Riemann sphere.

**Definition 4.7.** The *Fatou set* $F$ of $f$ is the largest open subset of $\hat{\mathbb{C}}$ such that the iterates $\{f^n\}$ are equicontinuous on that set.

**Definition 4.8.** The *Julia set* $J$ of $f$ is the complement of the Fatou set.

**Remark 4.9.** On the Fatou set, small neighborhoods tend to "stick together" and have the same limiting behavior. On the Julia set, small neighborhoods tend to "drift apart" and in a sense (Corollary 4.16) behave almost as chaotically as possible.

**Corollary 4.10.** *Attracting cycles are in $F$ and repelling cycles are in $J$.*

**Theorem 4.11.** *$F$ and $J$ are "completely invariant". If $x \in F$, then $f(x) \in F$ and $f^{-1}(x) \subset F$, and similarly for $J$.*

*Proof.* Follows from the definition. Adding or removing one function from the family does not change equicontinuity. □

**Theorem 4.12.** *If $\deg f \geq 2$, then $J$ is nonempty and infinite.*

*Proof.* First, assume that $J$ is empty. Then $\{f^n\}$ is equicontinuous on $\hat{\mathbb{C}}$, so we can use a variant of the Arzela-Ascoli theorem to say that a subsequence $(f^{n_i})$ converges to a rational map $R$. Since the degree function is continuous ([6]), $\deg(f^{n_i}) \to \deg R$. However, the left side diverges to $\infty$, which is a contradiction because the right side is finite. Thus, we have at least one point $z_0 \in J$.

Next, assume the complete orbit of $z_0$ is finite. If $\deg f \geq 2$, then we know each point in the orbit has to be a critical point, since otherwise it would have 2 or more preimages. However, then it would form an attracting cycle (since the derivative of the map at the critical point is 0), which means it would be in $F$. Thus, the complete orbit is infinite, so $J$ is infinite. □

**Remark 4.13.** Note that the previous result is not true for $F$. The *Lattés map*

$$z \mapsto \frac{(z^2+1)^2}{4z(z^2-1)}$$

has an empty Fatou set [6].

Let's take a look at what the Julia set for one of our logistic map equations looks like. For $f_{3.2}$, we know the repelling fixed points at $x = 0$ and $x = \frac{11}{16}$ are in $J$, and since $f(1) = 0$, $1 \in J$. What about complex-valued inputs?

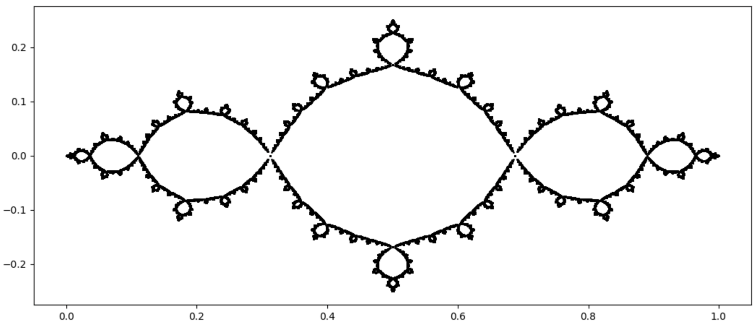


FIGURE 18. Computer-generated Julia set for $f_{3.2}$ in the complex plane.

Wow.

Before we prove Theorem 2.9, we need one last fact about critical points.

**Theorem 4.14.** *$z$ is a critical point of $f \iff f$ is not locally injective at $z$.*

*Proof.* If $f'(z) = \lambda \neq 0$, then $f$ can be expanded locally as $f(z+h) \approx f(z) + \lambda h$, which is injective. If $f'(z) = 0$, then $f$ can be expanded locally as $f(z+h) \approx f(z) + ch^d$ for $d > 1$, which is a d-to-1 mapping and so is not injective. □

With all of that said, we're finally ready for the proof of Theorem 2.9.

*Proof of Theorem 2.9.* First, note that a critical point falling into an attracting $n$-cycle of $f$ is equivalent to a critical point falling into an attracting fixed point of $f^n$. Therefore, we only need to consider attracting fixed points instead of $n$-cycles. If our attracting fixed point happens to be a critical point, then we're done. Otherwise, consider a small ball $B$ around the fixed point. Since the Fatou set is open, we can choose to make this ball entirely in $F$.

Next, we can take a look at the preimage of $B$ under $f$. Note that any polynomial of degree $d$ is a $d$-to-1 mapping except at critical points. Assuming the preimage doesn't contain a critical point, the branches of this preimage are disjoint. Let us choose the branch of $f^{-1}$ that maps the fixed point to itself. We can then repeat this to form an infinite family $(f^{-n})$.

Note that by complete invariance $f^{-n}(B)$ contains none of the points in the Julia set. This means we can use an incredibly powerful theorem.

**Theorem 4.15.** *(Montel's Theorem, or the Fundamental Normality[6] Test) Any family of holomorphic functions on an open domain $D \subseteq \hat{\mathbb{C}}$ whose ranges all do not include at least three points is equicontinuous.*

*Proof.* Long. Included in [7]. □

This theorem can seem very counterintuitive since there is no analog for real functions. I highly recommend taking a moment to consider families of holomorphic functions to get a feel for it. For example, take the family $\{z^n\}$. It can be verified that any open domain $D$ that doesn't intersect the unit circle $z = e^{i\theta}$ is

[6] "Normal" in this context means equicontinuous on compact sets. I have avoided using it in this paper because it is perhaps the most overloaded word in mathematics.

equicontinuous with respect to the spherical metric. However, if $D$ intersects the unit circle, then the family is no longer normal, and so $\bigcup_{n=0}^{\infty} D^n$ ends up being almost the entirety of $\hat{\mathbb{C}}$, with the only possible exceptions being 0 and $\infty$ if they are not included in $D$.

In fact, there is a straightforward corollary of Montel's theorem.

**Corollary 4.16.** *("Stuff Goes Everywhere"[7]) If $W$ is an open set that contains at least one point in $J$ then*

$$\bigcup_{n=0}^{\infty} f^n(W)$$

*contains every point in $\hat{\mathbb{C}}$ with at most two exceptions.*

*Proof.* Since $W$ intersects the Julia set, $R^n$ must not be equicontinuous on $W$. Therefore, the images of $f^n$ cannot exclude three or more points in the complex plane. □

Returning to our proof, since every $(f^{-n})$ misses the Julia set, which contains at least three points, they form an equicontinuous family. However, if our fixed point is $z_0$ it follows from the Chain Rule that

$$\begin{aligned} 0 < |f'(z_0)| &= \lambda < 1 \\ |(f^{-1})'(z_0)| &= \lambda^{-1} \\ |(f^{-n})'(z_0)| &= \lambda^{-n} \to \infty \end{aligned}$$

which contradicts equicontinuity. By this contradiction, a critical point must be in the basin of attraction. □

## 5. The Mandelbrot Set

We are slowly inching back towards the question of which values of $r$ cause $f_r$ to have an attracting cycle. However, now we can include complex values of $r$. To make things easier, we'll conjugate our map again.

**Theorem 5.1.** *A map of the form $f_r(x) = rx(1-x)$ with $r > 2$ is conjugate to exactly one map of the form $q_c(z) = z^2 + c$ with $c = \frac{r}{2} - \frac{r^2}{4}$.*

*Proof.* Verify that with $T : z \mapsto -rz + \frac{r}{2}$ we have that

$$q_c = T \circ f_r \circ T^{-1}.$$

□

Since 0 is the only critical point of $q_c$, by Theorem 2.9, we only need to look at the forward orbit of 0 to find an attracting cycle. Consider the set

$$M' = \{c \in \mathbb{C} \mid 0 \text{ falls into an attracting cycle of } q_c\}. \tag{5.2}$$

This set ends up being annoying to work with, so we can consider the similar set

$$M = \{c \in \mathbb{C} \mid \text{the forward orbit of 0 under } q_c \text{ stays bounded}\}. \tag{5.3}$$

The set $M$ is called the *Mandelbrot set.* $M$ is similar to $M'$, and it can be seen that $M' \subset M$, but $M$ also contains points like $i$ where the orbit of 0 is periodic but not attracting.

[7]Named by mathematics YouTuber 3Blue1Brown.

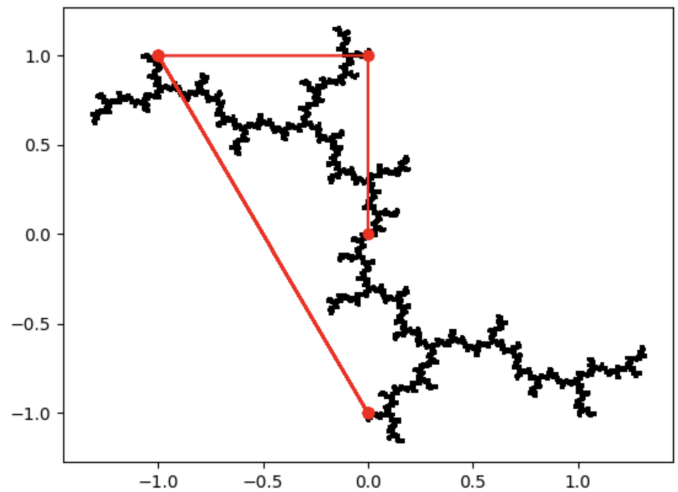


FIGURE 19. Julia set and forward orbit of 0 for $z \mapsto z^2 + i$.

The definition is equivalent to 0 being in the *filled Julia set*.

**Definition 5.4.** The *filled Julia set* $K$ is the set of all points that remain bounded under iteration. It includes the Julia set and bounded components of the Fatou set.

What does $M$ look like?

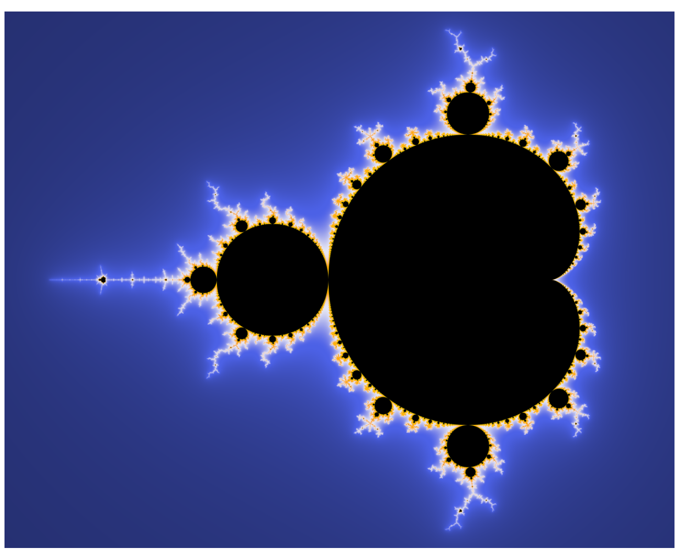

FIGURE 20. The Mandelbrot set (black region). Color added for dramatic effect.[8] [8]

Wow. Let's zoom in.

[8]Not really. The color represents the *escape time* for points in $M^C$. Blue points diverge faster than orange points.

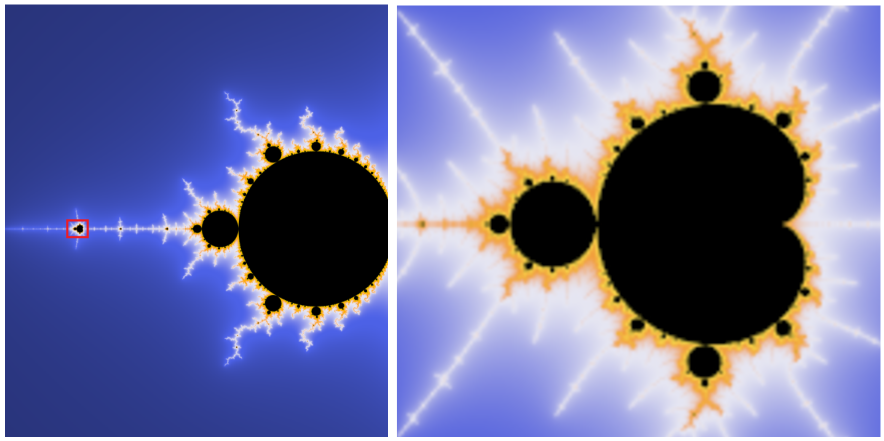

FIGURE 21. Right plot is a scaled version of the left plot.

It's a small copy of our Mandelbrot set! To find out what's so special about this location, we can use Theorem 5.1 and plot the special points of the logistic map on our Mandelbrot set.

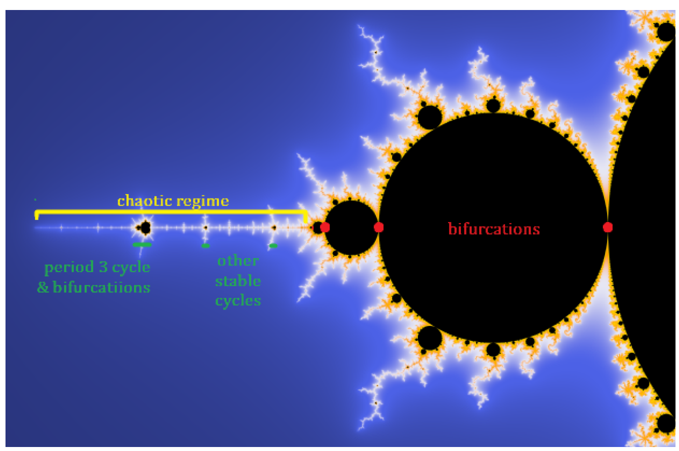


FIGURE 22. Notable points.

It seems like our mini-Mandelbrot corresponds somehow to the period 3 cycle! In fact, there is a general connection between attracting periodic cycles and homeomorphisms of the Mandelbrot set, and we can use renormalization to study these attracting cycles. Specifically, in analogy with the real case, we can define a renormalization operator that sends a neighborhood of points to a family of quadratic-like maps.

In this case, our renormalization just consists of picking the right domain $U$. We don't need to worry about rescaling since it doesn't affect the dynamics. These quadratic-like maps are not conjugate to any quadratic polynomial. However, they can get pretty close. For complex functions $f$ that are not necessarily conformal we can define two operators called the Wirtinger derivatives:

$$\partial f = \frac{1}{2}\left(\frac{\partial f}{\partial x} - i\frac{\partial f}{\partial y}\right),$$
$$\bar{\partial} f = \frac{1}{2}\left(\frac{\partial f}{\partial x} + i\frac{\partial f}{\partial y}\right).$$

If $f$ is conformal then by the Cauchy-Riemann equations we have that $\partial f = f'$ and $\bar{\partial} f = 0$. We can check if any function satisfies the *Beltrami equation* for some $\mu(z)$:

$$\bar{\partial} f = \mu(z)\partial f.$$

For any conformal map, $\mu = 0$ everywhere. If $\mu \neq 0$, then it measures how far a function is from being conformal. The case we're interested in is

**Definition 5.5.** A function $f$ is *quasiconformal* if it satisfies the Beltrami equation and $|\mu|_{\sup} < 1$.

Conformal maps send small circles to small circles. Quasiconformal maps send small circles to small ellipses with bounded eccentricity.

We can do slightly better than just replacing our Möbius transformations with quasiconformal maps, though.

**Definition 5.6.** Two quadratic-like maps $g$ and $h$ are *hybrid equivalent* if there exists a quasiconformal map $\phi$ such that $\phi \circ g \circ \phi^{-1} = h$ and $\bar{\partial}\phi = 0$ almost everywhere on the filled Julia set of $g$.

These hybrid equivalences turn out to be just rigid enough to give us an incredibly useful result first stated in [9].

**Theorem 5.7.** *(the Straightening Theorem) Every quadratic-like map is hybrid equivalent to a unique quadratic polynomial up to (conformal) conjugacy.*

We call the map $\chi$ that sends a quadratic-like map to its hybrid-equivalent quadratic of the form $z^2 + c$ the *straightening map*. With this, we can state our most powerful universality result. Consider a family $\mathbf{f} = \{f_\lambda : U_\lambda \mapsto U'_\lambda\}$ of quadratic-like maps, where $\lambda$ is a parameter in some closed Jordan disk $\Lambda$ (a subset of the parameter space homeomorphic to the closed unit disc with a boundary that is a Jordan curve). Suppose this family satisfies the following conditions:

- The disks $U_\lambda$ and $U'_\lambda$ move holomorphically over $\lambda$
- The family is *proper* in that $f_\lambda(0) \in \partial U'_\lambda$ for all $\lambda \in \partial\Lambda$.
- The family is *unfolded* in that the critical value $f_\lambda(0)$ winds once around 0 as $\lambda$ goes around $\partial\Lambda$.

In this case, we can define a *Mandelbrot-like set* $M_\mathbf{f} \subseteq \Lambda$ as the set of all $\lambda$ such that 0 is in the filled Julia set of $f_\lambda$, which for quadratic-like maps means the set of all points that stay within $U$ under iteration. Then

**Theorem 5.8.** *There exists a homeomorphism of $\Lambda$ onto a neighborhood of $M$ that coincides with a homeomorphism of $M_\mathbf{f}$ onto $M$. Moreover, this homeomorphism is given exactly by the straightening map $\chi$ and is conformal on int $M$ and quasiconformal on $\Lambda \setminus M$.*

Ths result is given in [10]. This shows that the Mandelbrot set is "universal" in the sense that any other Mandelbrot-like set is topologically equivalent to $M$.

Just as in the real case, if a $q_c$ has an attracting $k$-cycle, then $q_c^k$ can be renormalized to a quadratic-like map with a suitable choice of domain. Note that we're ignoring the "scaling" factor in the real case, since it doesn't affect the dynamics. We can define

**Definition 5.9.** A *hyperbolic* component $H$ of int $M$ is one where every parameter $c \in H$ has an attracting cycle.

If we apply this renormalization procedure and then straighten, we get a new map $\tilde{\chi}$ that sends $q_c$ in some hyperbolic component to a different $q_{c'}$. The *center* of this hyperbolic component is the value $c_0$ that will be mapped by $\tilde{\chi}$ to 0. The behavior of the Mandelbrot set around the hyperbolic components depends specifically on the value $c_1$ such that $\tilde{\chi}(q_{c_1}) = q_{\frac{1}{4}}$.

**Definition 5.10.** If $c_1$ borders a hyperbolic component other than the one with center $c_0$, then it is a *satellite* component. Otherwise, it is a *primitive* component.

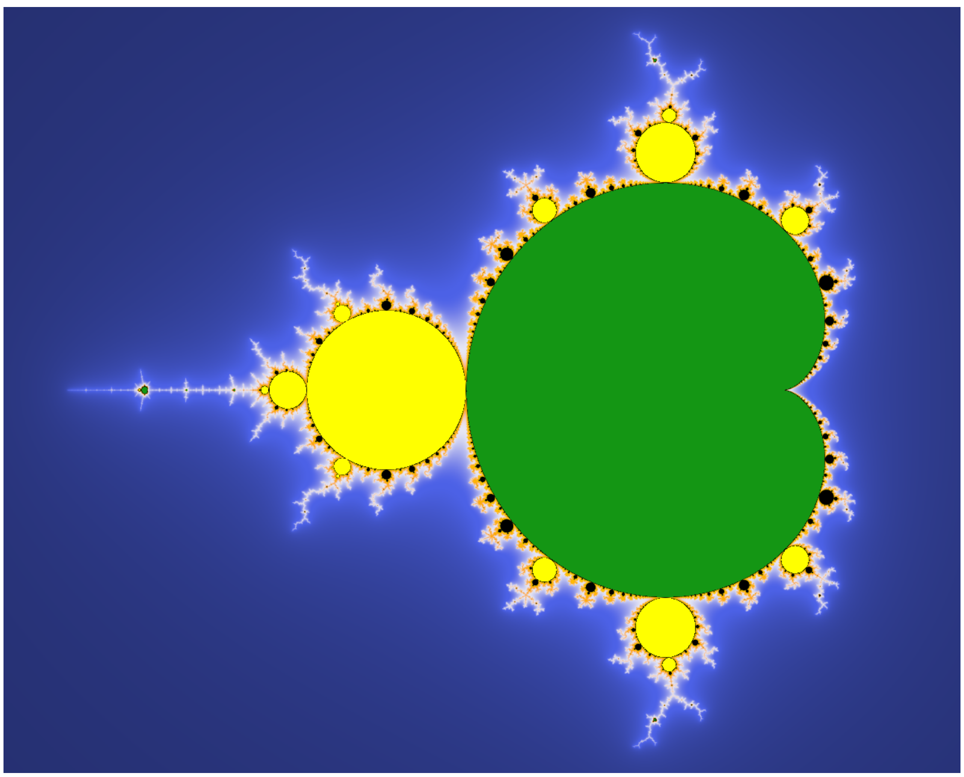

FIGURE 23. Examples of primitive (green) and satellite (yellow) components.

**Theorem 5.11.** *(Tuning Theorem for primitive components) If $W$ is a primitive component of $M$, then there exists a closed Jordan disk $\Lambda$ in a neighborhood of $W$ such that renormalizations of $\{q_c \mid c \in W\}$ form a Mandelbrot-like family. Thus, $W$ is homeomorphic to $M$ by the $\chi$, and this homeomorphism is conformal on int $M$ and quasiconformal on $\Lambda \setminus M$.*

The crux of the proof is in the construction of suitable $U_c$, $U_c'$, and $\Lambda$, which relies on the theory of *external rays*. This construction is only possible for quadratic-like maps, since for polynomial-like maps of higher degree (defined analogously), the filled Julia sets depend discontinuously on the parameter. It's therefore impossible to choose the $U_c$ so they vary holomorphically. Details of the proof can be found in [11] and[12], with a proof of conformality and quasiconformality in [13].

**Theorem 5.12.** *(Tuning Theorem for satellite components) If $W$ is a satellite component of $M$, then there exists a Jordan disk $\Lambda$ in a neighborhood of $W \setminus c_1$ such that $\tilde{\chi}$ induces a homeomorphism between $M_f$ and $M - \{\frac{1}{4}\}$.*

This proof is very similar to the previous one. Together, these let us get a very clear picture of the self-similarity of the Mandelbrot set.

## 6. The MLC Conjecture

Despite all that we can say about the structure of the Mandelbrot set, there's one question about it that has eluded mathematicians so far, and it has become one of the most important open problems in complex dynamics.

**Conjecture 6.1.** *(The MLC conjecture) The **M**andelbrot set is **l**ocally **c**onnected.*

This last section is intended to provide a survey of implications and partial results regarding the MLC conjecture. Here are some interesting implications.

**Theorem 6.2.** *(Density of Hyperbolicity) MLC $\implies$ $M'$ (as defined in 5.2) is exactly the interior of $M$.*

*Proof.* Requires almost 200 pages of background. Given in [14]. □

**Theorem 6.3.** *$MLC \iff$ a homeomorphism $f : \hat{\mathbb{C}} - D \to \hat{\mathbb{C}} - M$ extends to give a computable Fourier series for the boundary of $M$.*

*Proof.* The Laurent series for this map $f$ is known, proven and given in [15].

$$f(z) = z + \sum_{n=0}^{\infty} b_n z^{-n} = z - \frac{1}{2} + \frac{1}{8}z^{-1} - \frac{1}{4}z^{-2} + \cdots \tag{6.4}$$

The Fourier series would then be given by $f(e^{i\theta})$. The double implication is a consequence of the Carathéodory-Torhorst theorem. □

This result is particularly impressive because

**Theorem 6.5.** [16] *The boundary of $M$ has Hausdorff dimension 2.*

The Lebesgue measure is still unknown, but in a sense it's as complicated as a boundary in the plane can be. The last section of this paper will detail some partial results towards MLC.

**Theorem 6.6.** *The Mandelbrot set is connected.*

*Proof.* Follows from (6.4), but first we need two lemmas.

**Lemma 6.7.** *$M$ is compact*

*Proof.* It suffices to show that $M$ is closed and bounded in $\mathbb{C}$. To see that it is bounded, note that if $|c| > 2$ then the forward orbit of 0 under $q_c$ tends to $\infty$, so $M$ is a subset of the closed ball $|c| \leq 2$.

To see that it is closed, consider $q_c^n(0)$. This will always be a polynormial in terms of c. For example,

$$\begin{aligned} q_c(0) &= c, \\ q_c^2(0) &= c^2 + c, \\ &\vdots \\ q_c^{n+1}(0) &= (q_c^n(0))^2 + c. \end{aligned}$$

Denote $P_n(c) = q_c^n(0)$. $c \in M^C$ is equivalent to there being an $n$ such that $|P_n(c)| > 2$. Thus, if $W = \{z \in \mathbb{C} \mid |z| > 2\}$, we can write

$$M^C = \bigcup_{n=1}^{\infty} P_n^{-1}(W),$$

which is the union of open sets. Therefore, $M^C$ is open, which implies that $M$ is closed. □

**Lemma 6.8.** *If the complement $E$ of a simply connected subset of $\hat{\mathbb{C}}$ is compact, then it is connected.*

*Proof.* Since $E$ has $n > 1$ connected components, all of which are compact, we can use stereographic projection to send one of the components to a neighborhood around $\infty$. We then have $n - 1$ connected components in the plane whose complement is simply connected. Since each of the components has an open neighborhood that is disjoint from the others, it's easy to draw a loop inside both one of the neighborhoods and $E^C$ that can't be contracted to a point, which is a contradiction. □

**Remark 6.9.** The "compact" requirement is not necessary. In fact, some sources in complex analysis *define* simple connectedness as having a connected complement in $\hat{\mathbb{C}}$.[9]

Since $\hat{\mathbb{C}} - M$ is homeomorphic to $\hat{\mathbb{C}} - D$ by (6.4) and therefore simply connected, $M$ is connected. □

Our next result connects the MLC conjecture to renormalization.

**Theorem 6.10.** *(Yoccoz) The Mandelbrot set is locally connected at all points that are not infinitely renormalizable.*

This result is found in [17]. By Theorem 5.7 any point in a hyperbolic component is finitely but not infinitely renormalizable. An example of an infinitely renormalizable component is the *Feigenbaum parameter* $c = -1.401155\ldots$, which corresponds to the logistic map with $r = 3.56995\ldots$. This function was on the stable manifold, so iterations always stayed in the domain of the renormalization operator. For all real values of $c$, though, we also have a partial result in the style of Theorem 6.2.

[9]This is so they can partake in the time-honored tradition of hand-waving away the full proof as "algebraic topology mumbo jumbo". This tradition will be honored here.

**Theorem 6.11.** [18] *Hyperbolic parameters are dense in* $[-2, \frac{1}{4}]$ *on the real line. Equivalently, the values of* $r$ *such that* $f_r$ *has an attracting cycle form an open and dense set in* $[0, 4]$

Despite the regime past the Feigenbaum parameter seeming "chaotic", there is actually an open, dense set of non-chaotic periodic parameters.

There are more parameters where $M$ is known to be locally connected. However, despite all of this progress, the full MLC conjecture remains a mystery.

## Acknowledgments

I would like to thank my mentor DeVon Ingram for the endless insights and flexibility with meeting times, as well as for recommending complex dynamics as a topic. I felt like I left every meeting having learned something I didn't know existed beforehand. I would also like to thank Professor May for organizing the REU and allowing me to present a portion of what would become this paper as a talk during the program. Finally, I would like to thank fellow REU participant Alice Wang for giving feedback and helping to edit an early draft of this paper. As a result, I take no responsibility for any mistakes.[10]

All images not cited are my own work.

## References

[1] Collet, P., Eckmann, J.P. & Lanford, O.E. Universal properties of maps on an interval. Commun.Math. Phys. 76, 211–254 (1980). https://doi.org/10.1007/BF02193555

[2] Lanford, O. E. A computer-assisted proof of the Feigenbaum conjectures, Bull. AMS N. S.6:127 (1984). https://doi.org/10.1090/S0273-0979-1982-15008-X

[3] Eckmann, JP., Wittwer, P. A complete proof of the Feigenbaum conjectures. J Stat Phys 46, 455–475 (1987). https://doi.org/10.1007/BF01013368

[4] `(CC BY-NC; Ümit Kaya)`

[5] `GKFXtalk, de:User:Bjoern_klipp, CC BY-SA 3.0 <http://creativecommons.org/licenses/by-sa/3.0/>, via Wikimedia Commons`

[6] Beardon, A.F. Iteration of Rational Functions: Complex Analytic Dynamical Systems (1991).

[7] Gamelin, T. W. Complex Analysis (2001). https://doi.org/10.1007/978-0-387-21607-2

[8] `Wikimedia Commons (public domain)`

[9] Douady, A., & Hubbard, H. On the dynamics of polynomial-like mappings, Ann. Sci. Ecole Norm. Sup. (4) 18 (1985) 287-343.

[10] Lyubich, M. Baby Mandelbrot sets, renormalization and MLC. Gaz. Math. No. 113 (2007), 45–50.

[11] Douady, A. Chirurgie sur les applications holomorphes (2010).

[12] Haïssinsky, P. Modulation dans l'ensemble de Mandelbrot (2000). In T. Lei (Ed.), The Mandelbrot Set, Theme and Variations (pp. 37–66). chapter, Cambridge: Cambridge University Press.

[13] Lyubich, M. Feigenbaum-Coullet-Tresser universality and Milnor's hairiness conjecture. Annals of Mathematics. Second Series 149.2 (1999): 319-420.

[14] Douady, A., Hubbard, J. Exploring the Mandelbrot set. The Orsay Notes (1984-5).

[15] Ewing, J. H., Schober, G., The area of the Mandelbrot set, Numer. Math., vol. 61 (1992), pages 59-72.

[16] Shishikura, M. The Hausdorff Dimension of the Boundary of the Mandelbrot Set and Julia Sets. Annals of Mathematics, 147(2), 225–267 (1998). https://doi.org/10.2307/121009

[17] Hubbard, J.H. Local connectivity of Julia sets and bifurcation loci: three theorems of J.-C. Yoccoz (1993).

[18] Graczyk, J. Światek, G. Generic hyperbolicity in the logistic family, Ann. of Math. 146 (1997), 1–52 https://doi.org/10.2307/2951831

[10] Not true.